Desalination and Water Treatment
www.deswater.com

doi: 10.5004/dwt.2022.28609

265 (2022) 124–133
July

Recycling of waste chicken bones for greywater pollutants removal

Mohamed A. El-Khateeb[a,*], Hussein M. Ahmed[b], Neama A. Sobhy[b]

[a]*National Research Centre, Water Pollution Research Department, Dokki, Cairo, Egypt, Tel. +201003282503; email: elkhateebcairo@yahoo.com*
[b]*Housing and Building National Research Center, Egypt, HBRC, Sanitary Institute Environmental, Tel. +201065869112; email: hussein_fee@yahoo.com (H.M. Ahmed), Tel. +201156961368; email: neamaahmedreiad@yahoo.com (N.A. Sobhy)*

Received 27 January 2022; Accepted 27 May 2022

ABSTRACT

Treatment and reuse of wastewater can overcome the shortage and pollution of water resources. The separation of domestic wastewater into greywater and blackwater fractions can reduce the loads in a huge part of domestic wastewater. The goal of this study is to examine how activated carbon (CAB) made from chicken bones performs in the treatment of greywater. The physicochemical characteristics of raw and treated greywater were evaluated before and after treatment. The effect of ashing temperature (300°C and 550°C) of the carbon activated bone (CAB) was investigated. The ideal carbonization temperature was 550°C. The X-ray diffraction and scanning electron microscopy techniques are used to characterize the CAB particles. The batch adsorption process was done with different adsorbent doses and contact times. Different doses of chicken bone ash (CBA) were examined. The optimal CBA dosage at 60 min of contact time was 0.8 mg/L. The pseudo-second-order models were used to fit the kinetic experimental data. The removal rate obtained for chemical oxygen demand, PO_4, total Kjeldahl nitrogen, and total suspended solids was 95%, 96%, 97%, and 97% respectively. Meanwhile, with an R^2 of 0.99, the CBA's influence on batch adsorption was effectively represented by the Langmuir isotherm model. The CAB appears to be a potential adsorbent for the elimination of contaminants, according to the findings.

Keywords: Recycling; Reuse; Reduce; Valorization; Solid waste; Minimization

1. Introduction

Water resource degradation has become a severe environmental concern across the world. The increase in population rates along with the improvement in the daily life of people leads to a change in the volume and properties of wastewater. Water conservation and reuse are becoming increasingly crucial as serious problems include reduced groundwater and surface water levels, and droughts. Greywater is wastewater that hasn't been mixed with toilet effluents [1]. Separating home wastewater into black and greywater is an excellent way to avoid fecal contamination of greywater and save money on treatment [2]. Greywater usually contains low concentrations of nutrients compared to domestic wastewater. In particular, phosphorous in greywater may lead to eutrophication in water streams. The nitrogenous concentration in greywater is low (not mixed with urine). The kitchen is the primary source of nitrogen in greywater. The nitrogen content in greywater is influenced by nitrogen-containing cleaners and proteins in meat [3]. Nitrogen concentrations in mixed domestic greywater typically vary from 5 to 50 mg/L. Laundry detergents and dishwashing are the principal sources of phosphorus in greywater in countries where phosphorus-containing detergents are permitted. In areas where non-phosphorous detergents are used, average phosphorous values are typically between 4 and 14 mg/L [4]. Low nitrogen hinders the decomposition of organic compounds in the biological

* Corresponding author.

treatment process by reducing microbial activity. When untreated greywater is applied to soils, organic contaminants (oils and, fats) can plug infiltration beds or soil pores [3]. This danger must be addressed when constructing natural greywater treatment and reuse systems. Frequent monitoring and changes (adding nitrogen from alternative sources such as urine) are required for such systems to work properly. Greywater reuse has the potential to be quite important. Sequencing batch reactors (SBR) and membrane bioreactors (MBR) are two technologies that have proved their ability to produce treated effluent with high quality [5,6]. The expensive cost and lack of public knowledge, however, may limit their usage in small communities, particularly in rural parts of poor nations. Greywater treatment and reuse may be accomplished using a range of processes. To remove organic and pathogenic burdens from greywater, physical and biological procedures are required [7].

Various methods for treating greywater have been developed, including sorption, chemical treatment, ion exchange, membrane separation, electrolytic, and electro-dialysis [8]. Adsorption is still one of the most often used methods for removing pollutants from greywater due to its cheap cost and dependability. Wheat straw, sawdust, bone char, and sugarcane bagasse carbon have all lately received attention [9,10]. Animal bones are a type of biomass with little economic worth as solid waste. When animal bones are used as raw materials in charcoal production, their economic value rises significantly [11,12].

The adsorption approach has gotten a lot of attention compared to other treatment options. Adsorption has several advantages, including a low starting cost, a simple and adaptable design, the ability to reuse effluent, ease of operation, and insensitivity to harmful pollutants. Electrostatic processes, ion exchange, bonding interactions, and chemical reactions are the key mechanisms responsible for the removal of contaminants via the adsorption process. Activated carbon, for example, is a great absorbent for organic contaminants in the air, water, and soil. The outstanding properties of activated carbon, such as a mesoporous structure and huge surface area, are due to its adsorption ability [13,14].

Egypt has a large population, which increases the demand for food and chicken flesh is a favorite meal. Increased consumption of chicken meat leads to an increase in the accumulation of chicken bones as waste that is difficult to recycle [15].

The raw waste bone samples' X-ray diffraction (XRD) patterns revealed that the predominant component of the raw chicken bone samples was calcium hydroxyapatite, $[Ca_{10}(PO_4)\cdot 6(OH)_2]$ (HAP). Because hydroxyapatite is a bioceramic substance with a porous surface, it can operate as an adsorbent [16,17].

The core of this work is to study the performance of the chicken bones in the treatment of greywater. The investigation was broadened to include how pollutants are eliminated kinetically throughout the adsorption process.

2. Materials and methods

2.1. Chicken bone particles

Bones were collected from area homes. The bones were meticulously removed from the flesh, washed multiple times, and then boiled in distilled water for 4 h to eliminate lipids. The cleaning was carried out several times. The clean bones were then dried for 2 h at 105°C. Crushing, grinding, and sieving were applied to the dry bones to get 60–90 μm particle size.

2.1.1. Chicken bone ashing

A total of 50 g of dried chicken bones were ashed in the furnace at 300°C; and 550°C for 30 min. The dried and ashed bone was crushed in a mortar and sieved at a size no. 60–90 μm using a mesh analyzer. Furthermore, the surface characterization was carried out using the scanning electron microscope (SEM) technique.

2.2. Characterization of bone material

Both the dried and the ashed chicken bone were crushed with a mortar and sieved using a mesh analyzer at a size no. 60–90 μm. The bones were analyzed by SEM Model Quanta 250 FEG, (field emission attracted with accelerating gun) 30 KV, FEI Co. The approved PAN analytical computer software (X'Pert High Score Software 2006 – Module License: PW3209) with the aid of the International Center of Diffraction Database (PDF-2 Database/CD-Release 2005, N°. 9430 500 01611) received with the X-ray diffraction equipment (X'Pert Pro PAN analytical – Manufactured by PAN analytical B.V Co., The Netherlands (ISO 9001/14001 KEMA – 0.75160)).

2.3. Analysis of greywater

The pH/conductivity meter (WTW) was used to determine the pH values of raw and treated effluents. LoviBond digester (Model RD 125) and LoviBond photometer were used to determine the chemical oxygen demand (COD). The Kottrmann incubator was used to determine the biochemical oxygen demand (BOD). Determination of total Kjeldahl nitrogen (TKN), a Gerhardt distillator (Model Vapodest), and digester (Model Kieldatherm) were utilized. The shaker water bath (LabTech), and the mesh analyzer (Model) were used during the study. All analyses were performed in complying with APHA [18].

2.4. Adsorption study pattern

2.4.1. Contact time

To 1,000 mL of greywater, 1 g of chicken bone ash (CBA) was mixed thoroughly. The contact time ranged from 10 to 120 min. The Jar test procedures of stirring rate at 200 rpm for 20 s and 40 rpm for the remaining time of the experiment were carried out. The aliquots were then analyzed for COD, total suspended solids (TSS), turbidity, total phosphorus (TP), and TKN.

2.4.2. Adsorbent doses

Different doses of CBA 0.1, 0.2, 0.5, 0.8, and 1.0 g/L were tested. The same procedure was considered. At ambient temperature, 1,000 mL of greywater contained in a plastic beaker was stirred in an adsorption batch study. The

supernatant was filtered, and the filtrates were tested to assess the contents. The pH was ranging from 7.0 to 8.3.

2.5. Equilibrium sorption isotherms

Langmuir and Freundlich isotherm models were used to characterize the process equilibrium. To correlate the experimental results, the standard Freundlich and Langmuir models were applied. The Langmuir model implies monolayer adsorption, whereas the Freundlich model is empirical, assuming heterogeneous adsorption on the surface [19]. Eqs. (1) and (2) give the linear forms of the Freundlich and Langmuir models, respectively:

$$\log q_e = \log K_f + \frac{1}{n}\log C_e \tag{1}$$

$$\frac{1}{q_e} = \frac{1}{K_L q_{\max}} - \frac{1}{C_e} + \frac{1}{q_{\max}} \tag{2}$$

where q_e (mg/g) is the concentration of pollutant adsorbed/weight of CBA at equilibrium, C_e is the residual concentration of pollutants in the greywater at equilibrium (mg/L), q_m is the amount of pollutant adsorbed/unit of adsorbent (mg/g), K and n are Freundlich constants that could be calculated from the slope and intercept of the plots of each isotherm. While K is the Langmuir constant (L/mg) [19].

2.6. Evaluation of the kinetic process

In this study, kinetic models were used to characterize the behavior of the sorption process. Pseudo-first-order is commonly used during the sorption process [20]. This linear kinetic model is expressed using the following equation:

$$\log\left(q_e - q_t\right) = \log q_e - \frac{K}{2.303}t \tag{3}$$

The site occupancy is proportional to the square of the number of unoccupied sites. The pseudo-second-order chemisorption kinetic rate equation is as the following:

$$\frac{t}{q_t} = \frac{1}{Kq^2} - \frac{t}{q_e} \tag{4}$$

3. Results and discussion

3.1. Characterization of CBA

3.1.1. Surface morphology of the adsorbent

Fig. 1 presents the SEM analysis of the CBA before (a) and after (b) the treatment of greywater. The CBA contains crystalline structures with a rough and porous surface. Hence, there is evidence that the CBA can be used as an adsorbent [21].

At various magnifications, Fig. 2A depicts the CBA's irregular morphology (heterogeneous). The presence of pores with different shapes and sizes (micro., meso., and macropores) results in structural variability. Mesopores and macropores were discovered in the CBA. Mesopores can also be utilized to adsorb big molecules or when a quicker rate of adsorption is needed [14,22].

3.1.2. XRD elemental analysis of the CBA

Table 1 shows the structure of raw bone and the CBA before and after contact with greywater. The calcite decreases while hydroxyapatite increases gradually.

Figs. 3–5 depict the chemical properties of raw bone, CBA, and CBA following greywater treatment, respectively. The CBA showed transformation of calcite ($CaCO_3$) into hydroxyapatite ($Ca_{10}(OH)_2{\cdot}(PO_4)_6$) [22,23]. The CBA's phase purity and crystalline structural characteristics were evaluated using XRD (Figs. 3–5). The XRD analysis was used to investigate the crystal structure of the CBA. Additionally, the $CaCO_3$ was identified in the spectrum of the CBA and can be attributed to the dissolution of non-stoichiometric carbonate-containing apatite bone and assigned after burning to hydroxyapatite. A signal from $Ca_{10}(PO_4)_6(OH)_2$ was also seen. The diffraction patterns of the crystalline form of hydroxyapatite were also visible in the CBA's XRD data. The pattern of the bio-diffraction adsorbent is very similar to that of swine, animal bone meal, and bovine bones chars [22].

Fig. 1. (a) Dried chicken bones at 300°C and (b) chicken bones ashed at 550°C for 30 min (CBA).

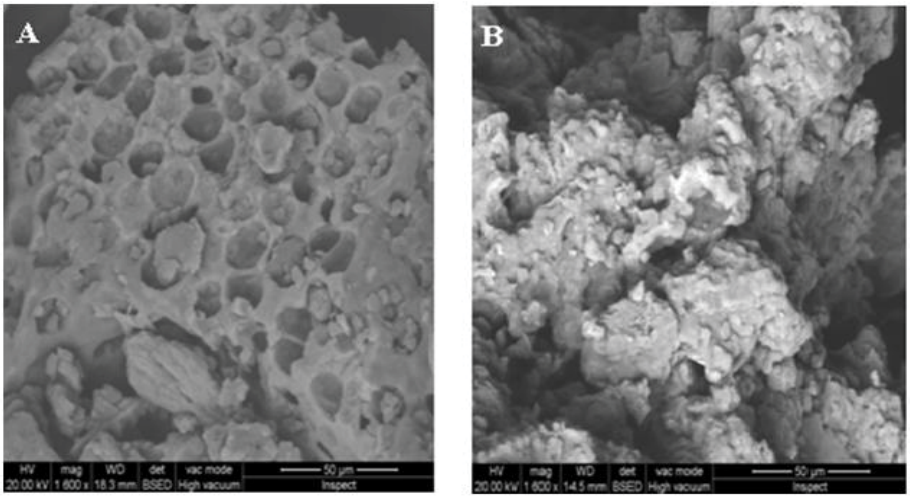

Fig. 2. SEM of the CBA (a) chicken bones ashed in the furnace at 550°C for 30 min (CBA) before treatment and (b) chicken bones ashed in the furnace at 550°C for 30 min (CBA) after treatment of greywater.

Table 1
Chemicals composition of raw bone, CBA before and after contact with greywater[a]

Item	XRD of raw bone	XRD of CBA at 550°C	XRD of CBA after treatment of greywater and burn at 550°C
Calcite ($CaCO_3$)	20	0	0
Hydroxyapatite ($Ca_{10}(OH)_2 \cdot (PO_4)_6$)	0	40	70

[a]Maximum count/s

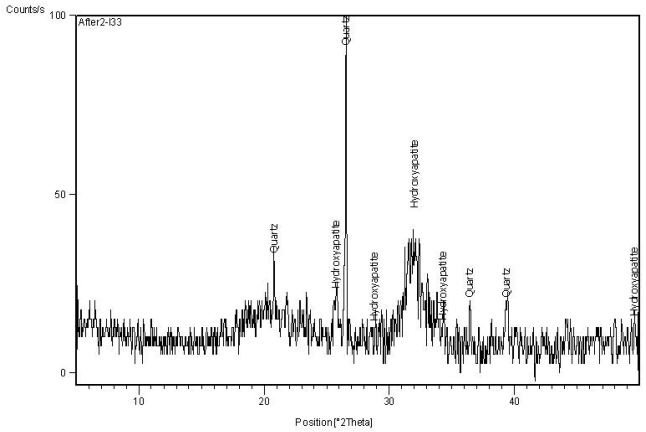

Fig. 3. XRD for the dried chicken crushed bones (of size 60–90 μm).

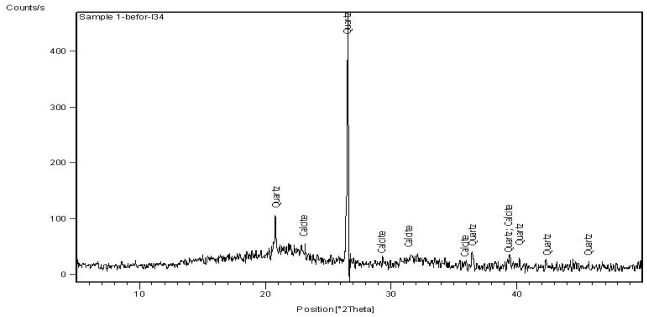

Fig. 4. XRD for the ashed chicken bones, CBA (550°C for 30 min, 60–90 μm) before treatment.

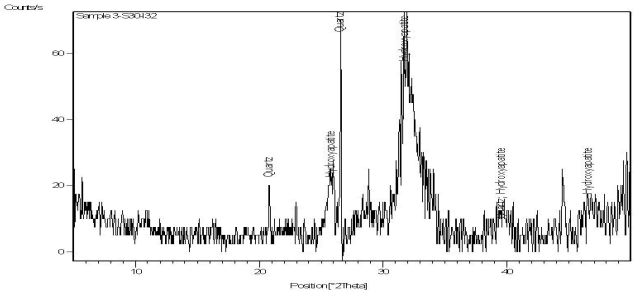

Fig. 5. XRD for the ashed chicken bones, CBA (550°C for 30 min, 60–90 μm) after treatment of greywater.

3.2. Selection of ashing temperature

The CBA at two different temperatures (300°C and 550°C) were examined for the treatment of greywater at a 0.5 g/L dose (Figs. 6 and 7). The Jar test procedures were followed (20 s at 200 rpm, 60 min at 40 rpm, and 30 min settling). All the pollutants were removed at different values. The ashed CBA at 550°C was highly efficient than that ashed at 300°C.

The adsorption of pollutants was high at 550°C. A recent study found that pollutants adsorption rises with

rising temperature, possibly because the physical interaction between adsorbate molecules and active sites of carbon surfaces is strong at high temperatures, resulting in increased adsorption of pollutants [23,24].

3.3. Effect of CBA dose

The influence of adsorbent dose on batch equilibrium research is an essential parameter since it reflects the sorbent–sorbate equilibrium of a system as well as the adsorption capabilities of the adsorbent. Different doses of CBA 0.10, 0.20, 0.50, 0.80, and 1.0 g/L were used for the removal of COD, BOD_5, TKN, TP, and TSS from greywater. The Jar test procedures were carried out (200 rpm for 20 s, 40 rpm contact time for 60 min, and 30 min settling). Fig. 8 depicts the *R*% of pollutants in relation to the adsorbent (CBA) dosage. The plots show that as the CBA dose was increased from 0.10 to 0.8 g/L, the clearance efficiency rose rapidly. The elimination efficiency indicated a small plateau between 0.8 and 1.0 g/L. All of the parameters investigated had the same adsorption pattern. This result may be attributed to the interwoven nature of these pollutants. The increase in removal capacity could be attributed to increasing the CBA dose, which resulted in more sorbent surfaces and hence more active sites for pollutant uptake. These findings were consistent with the trend of contaminants being removed by bone [25]. The adsorption process for COD and other contaminants approaches saturation with the addition of 0.8 g. The addition of increasing doses of adsorbent (CBA) causes stability in adsorption effectiveness because the contact surface area between the adsorbate and the adsorbent decreases throughout the adsorption process [26]. Because increasing the dose to 1.0 mg/L is not economically possible, the best adsorbent dose was 0.8 mg/L.

3.4. Effect of adsorption time

Fig. 9 shows the influence of contact time 10–120 min with 10 min intervals on the elimination of pollutants by CBA material. As previously stated, the experiment was done utilizing Jar test techniques. Fig. 9 shows the influence of contact time 10–120 min with 10 min intervals on the elimination of pollutants by CBA material. As previously stated, the experiment was done utilizing Jar test techniques. At the optimal dose of CBA 0.8 g/L, the adsorbent's efficiency was assessed at different contact times. The adsorption rate of contaminants increased fast at first

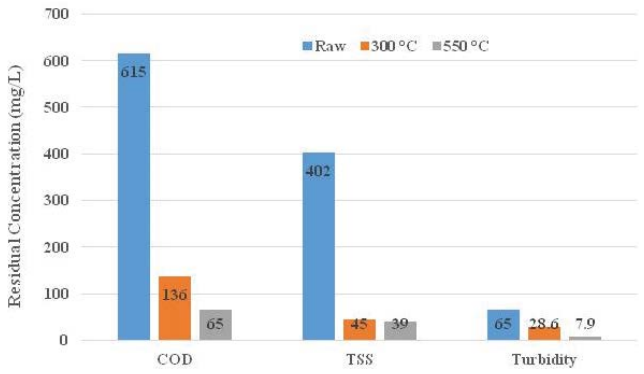

Fig. 6. Effect of ashing temperature (300°C, 550°C), on removal of TSS, COD, and turbidity (average of ten samples).

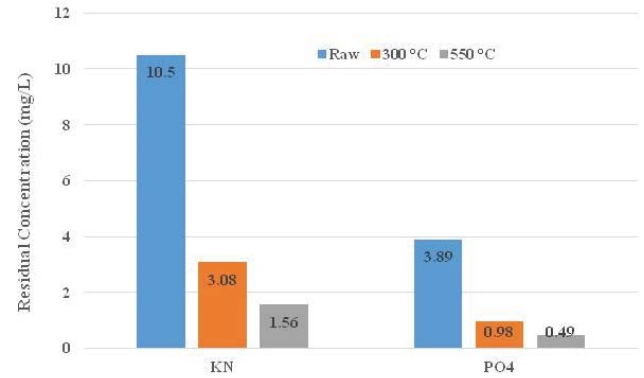

Fig. 7. Relationship between ash temperature (300°C, 550°C), and concentration of TKN, and PO_4 (average of ten samples).

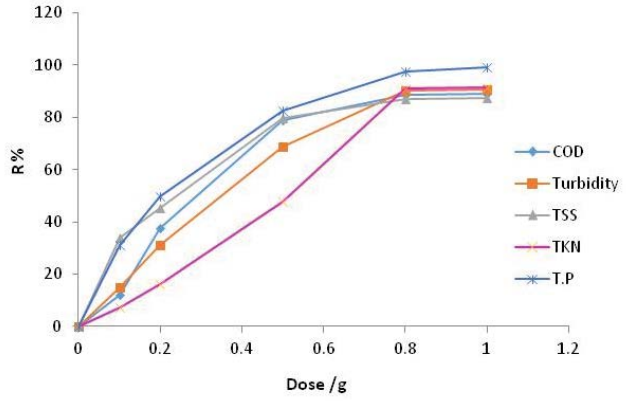

Fig. 8. Removal efficiency of the bone dose of CBA (0.10, 0.20, 0.50, 0.80, and 1.0 g/L) for removal of COD, TSS, TKN, TP, and turbidity (average of ten samples).

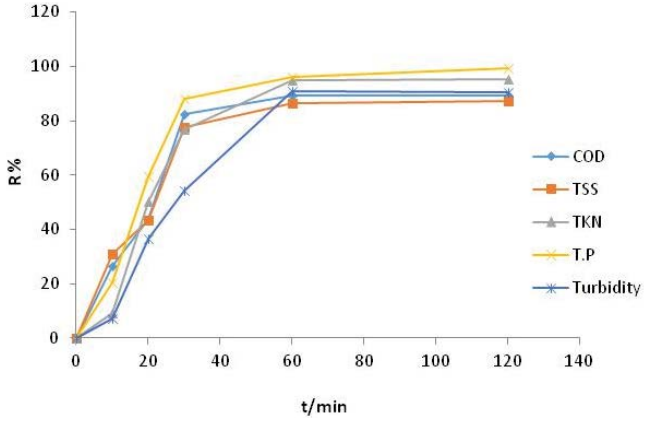

Fig. 9. Removal efficiency related to contact time 10 to 120 min at the optimum dose of bone ash (0.8 g/L) (average of ten samples).

contact time till reaching equilibrium adsorption at 40 min followed by a plateau between 60–120 min. Because the equilibrium phase had been reached, increasing the contact period did not result in a substantial change in adsorption [24]. As a consequence, 60 min was chosen as the ideal contact period for studying the kinetic removal of pollutants with the CBA.

3.5. Sorption characteristics

The sorption process of the adsorbent for COD, TSS, TKN, turbidity, and TP can be assessed by comparing the obtained results of equations of the adsorption isotherm [Eqs. (1) and (2)]. Table 2 shows the predicted parameters for the Freundlich and Langmuir sorption isotherms. These numbers show that both the Freundlich and Langmuir models suit the experimental data well. However, the Langmuir model (R^2 = 0.9909) is better matched to experimental data than the Freundlich isotherm (R^2 = 0.64434) in relation to the R^2 value for the CBA. The values of n in Table 2 are all bigger than 1.0. Using the correlation value, CBA calculates adsorption models for COD, TSS, TKN, turbidity, and TP (R^2). The correlation values of the two equations are compared in Table 2 [24]. The data are presented in Figs. 10–15.

Modeling the isotherm data with isotherm models is one of the basic requirements for the efficient design of

Table 2
Estimated parameters for Freundlich and Langmuir sorption isotherms, at the optimum dose of the CBA (0.8 g/L)

Parameter	Langmuir adsorption study		Freundlich adsorption study	
	R^2	q_{max}	R^2	N
COD	0.909	1,250	0.9066	2.5
TSS	0.946	2,500	0.9434	1.2
TKN	0.804	17.27	0.9422	1.4
Turbidity	0.788	120.48	0.7089	6.0
TP	0.967	588.24	0.5103	2.2

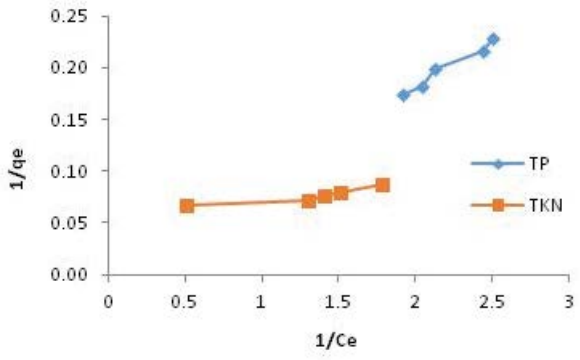

Fig. 10. Langmuir isotherm for TP, and TKN as affected by the CBA, at the optimum dose of 0.8 g/L.

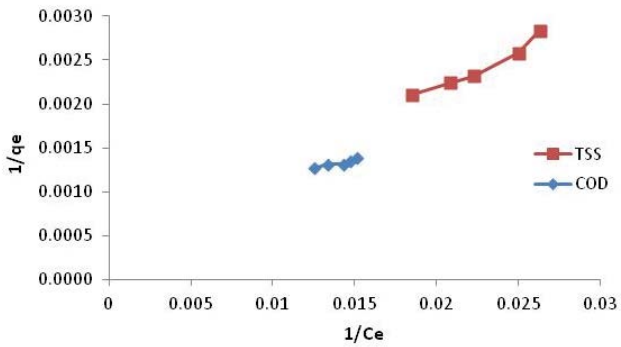

Fig. 11. Langmuir isotherm for TSS, and COD as affected by the CBA, at the optimum dose of 0.8 g/L.

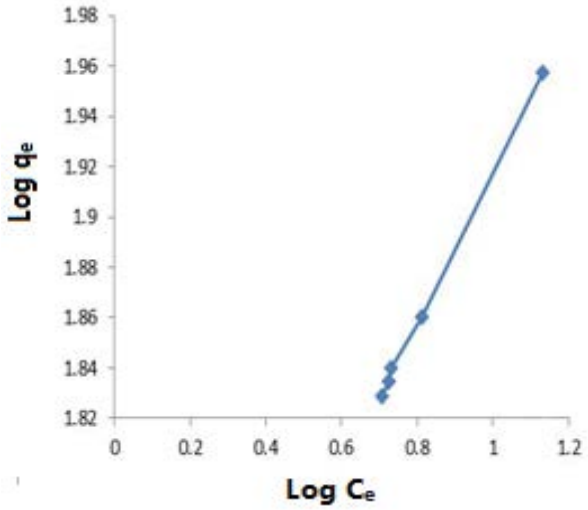

Fig. 12. Langmuir isotherm for turbidity as affected by the CBA, at the optimum dose of 0.8 g/L.

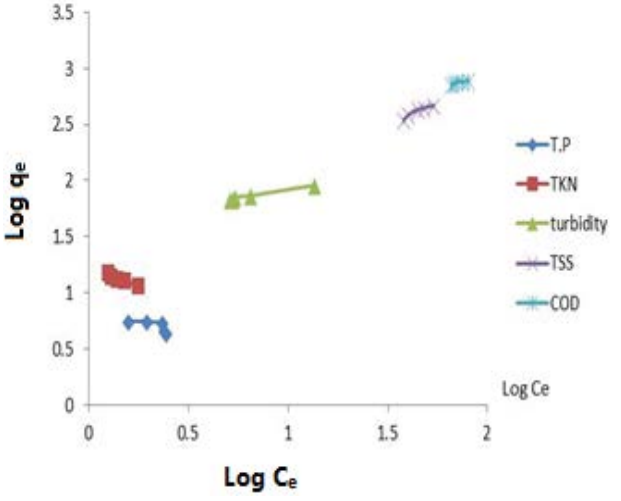

Fig. 13. Freundlich isotherm for turbidity, TP, and TKN as affected by CBA, at the optimum dose of 0.8 g/L.

adsorption treatment systems and the determination of q_m of an adsorbent for the target pollutant. In this study, four isotherm models were applied, and their compatibility with the isotherm data was analyzed: Langmuir, and Freundlich models. The Langmuir model [Eq. (1)] assumes that in adsorption systems, each pollutant molecule interacts with one active site located on the adsorbent surface (monolayer adsorption), and all the active sites located on the adsorbent are homogeneous and have equal binding energies. Thus, in the Langmuir model, adsorption is characterized as monolayer and homogeneous [13,14].

The q_m (mg/g) is a very important parameter in adsorption studies, denoting the maximum q_t of the adsorbent for the target pollutant. Freundlich equation [Eq. (2)] is an empirical isotherm model generally used to express multilayer and heterogeneous adsorption systems. Moreover, it supposes that the total adsorption energy exponentially decreases during adsorption. R^2 values of isotherm models applied in the present study are listed in Table 2. The highest R^2 values were found for the Langmuir model; thus, the adsorption of pollutants on the bone surfaces is consistent with the Langmuir model. These results indicate that the pollutants molecules are adsorbed on a monolayer of the homogeneous active sites [13,27].

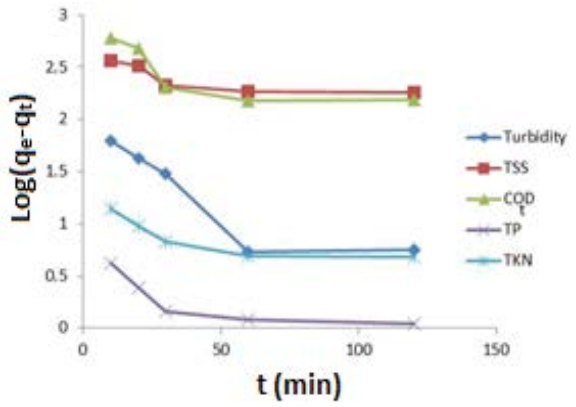

Fig. 14. First-order model for TKN, TP, COD, TSS, and turbidity as affected by the CBA at contact time 10 to 120 min.

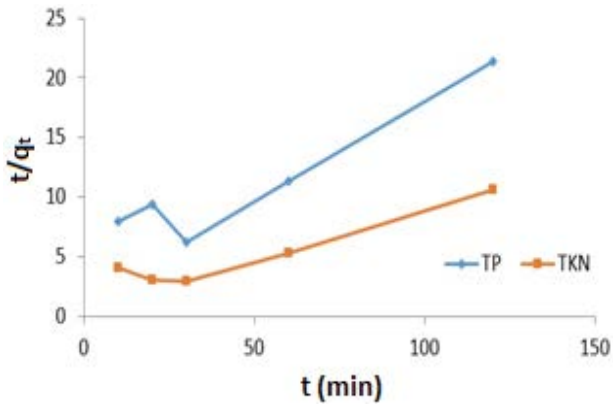

Fig. 15. Second-order model for TP, and TKN as affected by the CBA at contact time 10 to 120 min.

The adsorption of COD, TKN, TSS, turbidity, and TP using CBA follows the Langmuir adsorption isotherm pattern (Table 2). On the surface of the chicken bone ash adsorbent, the adsorbates COD, TKN, TSS, turbidity, and TP form a monolayer layer [26].

3.6. Kinetic study of CBA

Kinetic analysis is essential to evaluate the practical applicability of an adsorbent as it is useful for understanding the mechanism and rate of adsorption. In addition, the determination of a mathematical formula that can describe the kinetic reactions of an adsorbent–adsorbate system is necessary for the precise design of large-scale treatment processes [13,14,28].

To investigate the governing mechanism of adsorption processes such as mass transfer and chemical reaction, the pseudo-first-order and pseudo-second-order equations were employed to simulate the kinetics of pollutants removal onto the surface of the CBA powder [29]. Figs. 16 and 17 show straight-line plots of $\log(q_e–q_t)$ against time (t) to calculate the rate constant, k_1, and correlation coefficients, R^2. With the coefficient of 05902, 0.608, 0.6517, 0.7561, and 0.8226 for COD, TSS, TKN, turbidity, and PO_4^{3-}, respectively. As a result, when compared to the correlation coefficient, the adsorption of contaminants on the CBA surface did not follow pseudo-second-order kinetics.

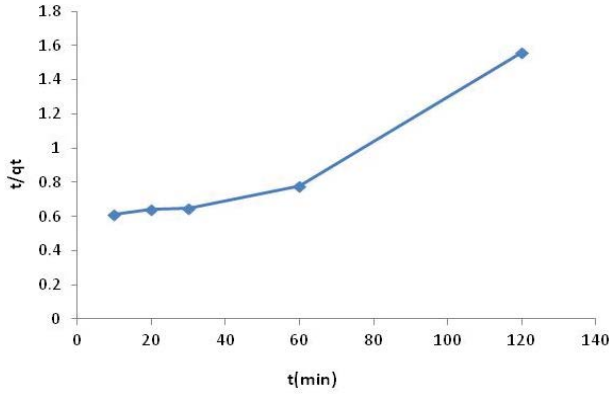

Fig. 16. Second-order model for turbidity as affected by the CBA at contact time 10 to 120 min.

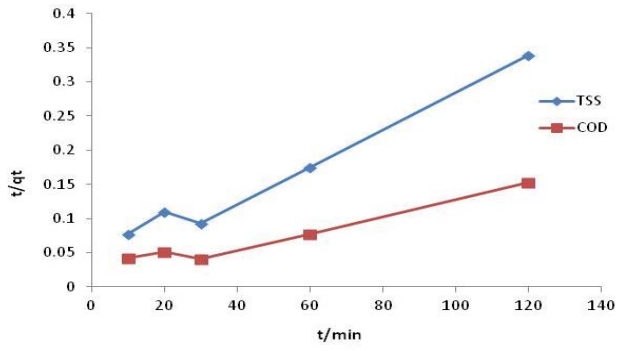

Fig. 17. Second-order model for COD, and TSS as affected by the CBA at contact time 10 to 120 min.

If pseudo-second-order kinetics were used, the plot of t/q_t vs. t should yield a straight line, and q_e, k, and h can be calculated from the slope and intercept of the plot, respectively. Figs. 1 and 2 illustrate the plot of the linearized form of the pseudo-second-order [30,31]. The pseudo-first-order and pseudo-second-order rate constants, as well as the related correlation coefficients, were determined in Figs. 16–20 and provided in Table 3.

The plot of t/q_t vs. t Figs. 18–20 show a standard set of straight lines, for the pseudo-second-order model, (correlation coefficient, with the coefficient of 0.9505, 0.9709, 0.9002, 0.9211 and 0.8920 for COD, TSS, TKN, turbidity, and PO_4^{3-}, respectively). The theoretical R^2 values for adsorption of CBA are based on the pseudo-second-order kinetic model. This presupposes that the rate-determining step is the chemisorption process. The COD, TSS, TKN, and turbidity chemisorb to the CBA surface by forming a chemical (covalent) bond, and they tend to choose areas with the highest coordination number. It was clear from the R^2 values obtained from plots of pseudo-first-order and pseudo-second-order rate equations that as the concentration of the adsorbate increases, the correlation of experimental data with the pseudo-second-order kinetics model increases while the correlation with the pseudo-first-order model reduces [29].

The mechanism governing the adsorption process, such as a chemical reaction, intra-particle diffusion, or mass transfer, was investigated using pseudo-first-order and second-order kinetics patterns. In order to characterize the kinetics of absorption, various formalisms have been established in the literature. Lagergren's model [22] yields the rate constant for first-order adsorption. Table 3 lists the constants of the kinetic models for the adsorption of contaminants by carbon activated bone (CAB). The findings revealed that the adsorption follows a pseudo-second-order model with an R^2 value indicating a good coefficient of determination and that experimental data may be changed to fit the model.

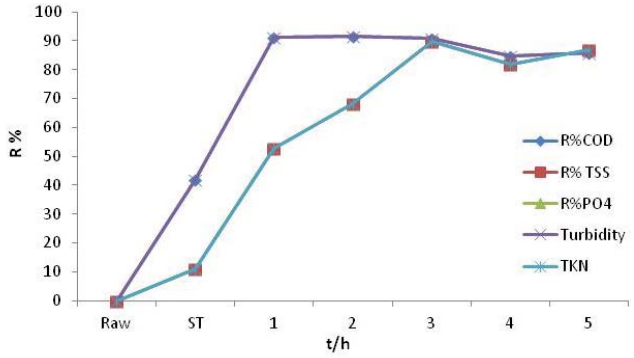

Fig. 18. Relation between R% of pollutants and time in column test at different contact time (1, 2, 3, 4, and 5 h), 2.5 mL/min flow rate, and 50 cm column height (average of ten samples).

Table 3
Estimated parameters for first-order and second-order kinetic study at contact time 10 to 120 min

	First-order	Second-order
	R^2	R^2
COD	0.5902	0.9505
TSS	0.608	0.9709
TKN	0.6517	0.9002
Turbidity	0.7561	0.9211
TP	0.8226	0.892

3.7. Column test and breakthrough curve

In continuous studies using bone, the CBA columns were used to investigate the removal capacity of pollutants at different contact times (1, 2, 3, 4, and 5 h) (Fig. 21 and Table 4). As seen by the R%, the pollutants' breakthrough curves were the inverse of their adsorption. After 3 h the pollutant breakthrough points were reached. The various contact periods revealed that increasing the contact time enhanced the adsorbents' adsorption capacity [32]. The flow rate was 2.5 mL/min, and the height of the column was 50 cm.

4. Conclusion

In this study, chicken bone ash was prepared and used as an adsorbent to remove pollutants from greywater. Characterization analyses reveal that chicken bone ash possesses unique properties and a high potential as an efficient adsorbent. In addition, these analyses showed that several characterization parameters, such as surface morphology, of the original chicken bone ash material were improved after its modification via the thermal process. According to the results of the Langmuir model, which fitted best with the experimental data, the R^2 of chicken bone ash for COD, TSS, TKN, turbidity, and TP was 0.909, 0.946, 0.804, 0.788, and 0.967. Furthermore, the kinetic study demonstrated that the experimental kinetic data at different COD, TSS, TKN, turbidity, and TP concentrations followed the pseudo-second-order kinetic model, the R^2 of chicken bone ash for COD, TSS, TKN, turbidity, and TP was 0.9505, 0.9709, 0.9002, 0.9211, and 0.892. Moreover, the optimum experimental condition for achieving the maximum chicken bone ash was as follows: temperature ash = 550°C. Based on the above results, it can be seen that the addition of chicken bone-based adsorbent can reduce the COD value in greywater by 74.45%; The TDS value of waste decreased by

Table 4
Concentration of pollutants at different steps in column test different contact time (1, 2, 3, 4, and 5 h), 2.5 mL/min flow rate, and 50 cm column height (average of ten samples)

	Breakthrough curve				
Test	COD	Turbidity	TSS	TKN	TP
Raw	619	69	375	11	4.12
ST	523	40	202	9.8	2.15
1	285	6.15	136	5.2	1.16
2	153	5.95	105	3.5	0.52
3	75	6.38	40	1.12	0.189
4	86	10.56	62	1.98	0.086
5	75	9.75	60	1.43	0

63.64% and 51.35%, respectively. Likewise, the TSS value in waste decreased by 66.67% and 46.15%, respectively.

The adsorbent from chicken bone ash characteristically contains apatite carbonate compound minerals and rough and porous surface morphology. Increasing the ashing temperature, contact time and doses of the adsorbent used will increase the adsorption performance. Chicken bone ash adsorbent can reduce levels of COD, turbidity, TSS, TKN, and TP and improve the quality of waste.

The application of CBA adsorbent can reduce the levels of pollutants in greywater.

Apatite carbonate compound minerals and a rough and porous surface shape were found in the CBA.

Increasing the ashing temperature, contact time and doses of the adsorbent used will increase the adsorption performance. The existence of calcium hydroxyapatite, $[Ca_{10}(PO_4)_6(OH)_2]$ (HAP), as a substantial component of the bone material was discovered by analysis.

Removal of COD, TKN, TSS, turbidity, and TP using CBA was carried out according to the Langmuir adsorption isotherm model. While the pseudo-second-order model describes the removal kinetics.

Data availability statement

All data, models, and code generated or used during the study appear in the submitted article.

References

[1] E. Eriksson, K. Auffarth, A.-M. Eilersen, M. Henze, A. Ledin, Household chemicals and personal care products as sources for xenobiotic organic compounds in grey wastewater, Water SA, 29 (2003) 135–146.
[2] S. De Gisi, P. Casella, M. Notarnicola, R. Farina, Greywater in buildings: a mini-review of guidelines, technologies and case studies, Civ. Eng. Environ. Syst., 33 (2016) 35–54.
[3] M. Salih, K.R. Reshma, K.R. Nandu, A.A. Salam, A.A. Akbar Shah, Domestic greywater treatment by natural coagulants combined with layered filter media, Int. Res. J. Eng. Technol., 7 (2020) 2620–2626.
[4] D.M. Ghaitidak, K.D. Yadav, Characteristics and treatment of greywater—a review, Environ. Sci. Pollut. Res., 20 (2013) 2795–2809.
[5] C. Merz, R. Scheumann, B. El Hamouri, M. Kraume, Membrane bioreactor technology for the treatment of greywater from a sports and leisure club, Desalination, 215 (2007) 37–43.
[6] A. Moawad, U.F. Mahmoud, M.A. El-Khateeb, E. El-Molla, Coupling of sequencing batch reactor and UASB reactor for domestic wastewater treatment, Desalination, 242 (2009) 325–335.
[7] M. Khalil, Y. Liu, Greywater biodegradability and biological treatment technologies: a critical review, Int. Biodeterior. Biodegrad., 161 (2021) 105211, doi: 10.1016/j.ibiod.2021.105211.
[8] A. Mahmoudi, S.A. Mousavi, P. Darvishi, Greywater as a sustainable source for development of green roofs: characteristics, treatment technologies, reuse, case studies and future developments, J. Environ. Manage., 295 (2021) 112991, doi: 10.1016/j.jenvman.2021.112991.
[9] M.A. Ahanger, N.S. Tomar, M. Tittal, S. Argal, R.M. Agarwal, Plant growth under water/salt stress: ROS production; antioxidants and significance of added potassium under such conditions, Physiol. Mol. Biol. Plants, 23 (2017) 731–744.
[10] L. Schneider, Greywater Reuse in Washington State, Rule Development Committee Issue Research Report Final, Washington State Department of Health-Wastewater Management Program, 2009, pp. 1–16.
[11] M. Khalil, M.A. Berawi, R. Heryanto, A. Rizalie, Waste to energy technology: the potential of sustainable biogas production from animal waste in Indonesia, Renewable Sustainable Energy Rev., 105 (2019) 323–331.
[12] M. Tripathi, J.N. Sahu, P. Ganesan, Effect of process parameters on production of biochar from biomass waste through pyrolysis: a review, Renewable Sustainable Energy Rev., 55 (2016) 467–481.
[13] G.A. Rumman, T.J. Al-Musawi, M. Sillanpaa, D. Balarak, Adsorption performance of an amine-functionalized MCM–41 mesoporous silica nanoparticle system for ciprofloxacin removal, Environ. Nanotechnol. Monit. Manage., 16 (2021) 100536, doi: 10.1016/j.enmm.2021.100536.
[14] M. Yilmaz, T.J. Al-Musawi, M.K. Saloot, A.D. Khatibi, M. Baniasadi, D. Balarak, Synthesis of activated carbon from *Lemna minor* plant and magnetized with iron(III) oxide magnetic nanoparticles and its application in removal of ciprofloxacin, Biomass Convers. Biorefin., (2022) 1–14, doi: 10.1007/s13399-021-02279-y.
[15] M.A. Mahmoud, H.S. Abdel-Mohsein, Health risk assessment of heavy metals for Egyptian population via consumption of poultry edibles, Adv. Anim. Vet. Sci., 3 (2015) 58–70.
[16] Y. Mikhaylova, G. Adam, L. Häussler, K.-J. Eichhorn, B. Voit, Temperature-dependent FTIR spectroscopic and thermoanalytic studies of hydrogen bonding of hydroxyl (phenolic group) terminated hyperbranched aromatic polyesters, J. Mol. Struct., 788 (2006) 80–88.
[17] K. Devarajan, S. Voigt, S. Shroff, S.G. Weiner, R.O. Wein, Diagnosing fish bone and chicken bone impactions in the emergency department setting: measuring the system utility of the plain film screen, Ann. Otol. Rhinol. Laryngol., 124 (2015) 614–621.
[18] APHA, Standard Methods for the Examination of Water and Wastewater, 23rd ed., American Public Health Association, Washington, DC, USA, 2021.
[19] M.A. El-Khateeb, Physico-chemical and kinetic evaluation of a combined vertical settler/self-aerated unit for wastewater treatment and reuse, CLEAN–Soil, Air, Water, 49 (2021) 2100147, doi: 10.1002/clen.202100147.
[20] M.C. Ncibi, B. Mahjoub, M. Seffen, Kinetic and equilibrium studies of methylene blue biosorption by *Posidonia oceanica* (L.) fibres, J. Hazard. Mater., 139 (2007) 280–285.
[21] E. Haluk, K. Yeliz, Ö. Orhan, Production of bone broth powder with spray drying using three different carrier agents, Korean J. Food Sci. Animal Resour., 38 (2018) 1273–1285.
[22] C. Djilani, R. Zaghdoudi, F. Djazi, B. Bouchekima, A. Lallam, P. Magri, Preparation and characterisation of activated carbon from animal bones and its application for removal of organic micropollutants from aqueous solution, Desal. Water Treat., 57 (2016) 25070–25079.
[23] A.R. Toibah, F. Misran, Z. Mustafa, A. Shaaban, S.R. Shamsuri, Calcium phosphate from waste animal bones: phase identification analysis, J. Adv. Manuf. Technol., 12 (2018) 99–110.
[24] N.A. Yusoff, N. Ngadi, H. Alias, M. Jusoh, Chemically treated chicken bone waste as an efficient adsorbent for removal of acetaminophen, Chem. Eng. Trans., 56 (2017) 925–930.
[25] A. Ramdani, S. Taleb, A. Benghalem, N. Ghaffour, Removal of excess fluoride ions from Saharan brackish water by adsorption on natural materials, Desalination, 250 (2010) 408–413.
[26] U. Hasanah, A. Iryani, A. Taufiq, D.A.D. Putra, Chicken bone based adsorbent for adsorption of Pb(II), Cd(II), and Hg(II) metals ion liquid waste, Helium: J. Sci. Appl. Chem., 1 (2021) 11–18.
[27] T.J. Al-Musawi, N. Mengelizadeh, O. Al Rawi, D. Balarak, Capacity and modeling of Acid blue 113 dye adsorption onto chitosan magnetized by Fe_2O_3 nanoparticles, J. Polym. Environ., 30 (2021) 344–359.
[28] T.A. Saleh, Isotherm, kinetic, and thermodynamic studies on Hg(II) adsorption from aqueous solution by silica-multiwall carbon nanotubes, Environ. Sci. Pollut. Res., 22 (2015) 16721–16731.
[29] P. Senthil Kumar, K. Kirthika, Equilibrium and kinetic study of adsorption of nickel from aqueous solution onto bael tree leaf powder, J. Eng. Sci. Technol., 4 (2009) 351–363.

[30] V. Skoulou, A. Zabaniotou, Investigation of agricultural and animal wastes in Greece and their allocation to potential application for energy production, Renewable Sustainable Energy Rev., 11 (2007) 1698–1719.
[31] M. Abdulredha, A.L.K. Rafid, D. Jordan, K. Hashim, The development of a waste management system in Kerbala during major pilgrimage events: determination of solid waste composition, Procedia Eng., 196 (2017) 779–784.
[32] A.P. Sasidharan, V. Meera, V.P. Raphael, Nanochitosan impregnated polyurethane foam in the removal of phosphate and coliforms from greywater, Nanotechnol. Environ. Eng., (2022) 1–12, doi: 10.1007/s41204-021-00214-0.